ACS Macro Letters

Letter

pubs.acs.org/macroletters

Amphiphilic Hybrid Nano Building Blocks with Surfactant-Mimicking Structures

Weikun Li, Srinivas Thanneeru, Istvan Kanyo, Ben Liu, and Jie He*

Department of Chemistry, University of Connecticut, Storrs, Connecticut 06269, United States

Supporting Information

ABSTRACT: We report the preparation and self-assembly of amphiphilic hybrid nano building blocks (NBBs) with surfactant-mimicking structures. These NBBs, composed of hydrophilic silica-like heads tethered with well-defined one or two hydrophobic polystyrene (PS) tails, were prepared by efficient intramolecular cross-linking via silane chemistry. Using a series of "AB" diblock copolymers (BCPs) and "ABA" tri-BCPs of PS and poly(*tert*-butyl acrylate-*co*-3-(trimethoxysilyl)propyl methacrylate) (P(*t*BA-*co*-TMSPMA)), the intramolecular self-folding of P(*t*BA-*co*-TMSPMA) blocks and the deprotection of *tert*-butyl groups were demonstrated to be an efficient method to prepare amphiphilic NBBs with a hydrophilic silica head tethered by one or two PS tails. The formation of NBBs was carefully studied by gel permeation chromatography, nuclear magnetic resonance spectroscopy, and transmission electron microscopy. The self-assembly of these amphiphilic NBBs was further investigated by fixing the molecular weight of PS tails and varying the size of hydrophilic heads. The intramolecular cross-linking of hydrophilic heads that shifted the hydrophilic/hydrophobic balance of polymers resulted in morphological transitions from bilayered vesicles to spherical micelles. Spherical micelles prepared from NBBs with large hydrophilic heads were found to have surface protrusions that differed from the self-assembly of linear BCPs. We also observed that the chain conformation of PS tails was critical for the self-assembly of NBBs, where the bitailed NBBs with highly stretched PS tails favored bilayered vesicle structures.

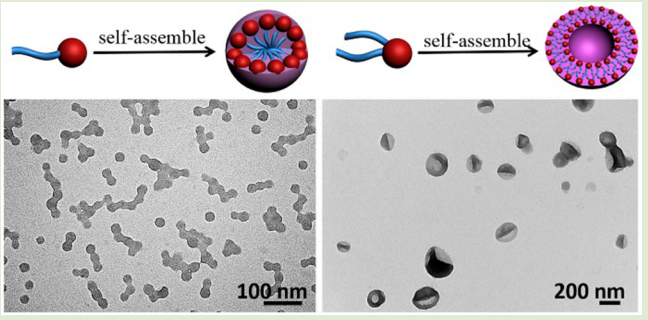

Nano building blocks (NBBs) composed of ultrafine nanoparticle cores tethered by flexible polymers have attracted much attention due to their applications in pharmaceutical technology and catalysis.[1−5] NBBs structurally analogous to surfactant molecules are engaged with many characteristics of molecular and colloidal amphiphiles; thus, they can stand out as a promising model to bridge the study of polymer synthesis and nanomaterials. Unlike bare colloidal particles, the interaction between NBBs is dominated by the nature of polymer tethers, e.g., chemical compositions, numbers, lengths, and locations on nanoparticle cores.[6−10] A couple of untraditional hierarchical assemblies and phase behaviors of NBBs have been observed in simulation studies by varying the polymer tethers.[11,12] Various nanostructures originating from the self-assembly of NBBs may have promising applications in functional materials and devices.[13−17] The engineering of polymer tethers is believed to enable the controlled self-assembly of NBBs at the single-chain level.[18−21] However, the experimental study of this new building block is still lacking,[22−31] especially in the observation of correlations between NBB nanostructures and their assemblies. This is mainly because of the great challenges in the synthesis of structurally well-defined NBBs, i.e., the manipulation of polymer tethers of NBBs at a molecular scale.[32]

We recently reported a new synthetic strategy to prepare hybrid NBBs with silica-like cores tethered by poly(ethylene oxide) (PEO).[33] This strategy was based on the intramolecular hydrolysis and polycondensation of silane moieties within individual block copolymer (BCP) chains. Using di-BCPs containing PEO and poly(3-(trimethoxysilyl)propyl methacrylate-*co*-methyl methacrylate) (P(TMSPMA-*co*-MMA)), we demonstrated that the intramolecular cross-linking of TMSPMA moieties could be used to prepare highly uniform, tadpole-shaped hybrid NBBs. The yielded NBBs had a silica-like hydrophobic head and a hydrophilic PEO tether as a result of the occurrence of hydrolysis and polycondensation reactions of TMSPMA moieties in the hydrophobic block. Unlike previously reported covalent cross-linking reactions, this approach allowed the efficient preparation of NBBs under mild conditions, and the obtained hybrid NBBs were highly uniform and easily visualized under a transmission electron microscope (TEM) because of high electron density. In this contribution, we expand the capacity of this method by mimicking natural surfactants having a hydrophilic head and one (or two) hydrophobic fatty tail(s). Our synthetic approach is summarized in Figure 1a. A series of "AB" di-BCPs and "ABA" tri-BCPs of polystyrene (PS) and poly(*tert*-butyl

Received: May 15, 2015
Accepted: June 25, 2015
Published: June 30, 2015

DOI: 10.1021/acsmacrolett.5b00321
ACS Macro Lett. 2015, 4, 736−740

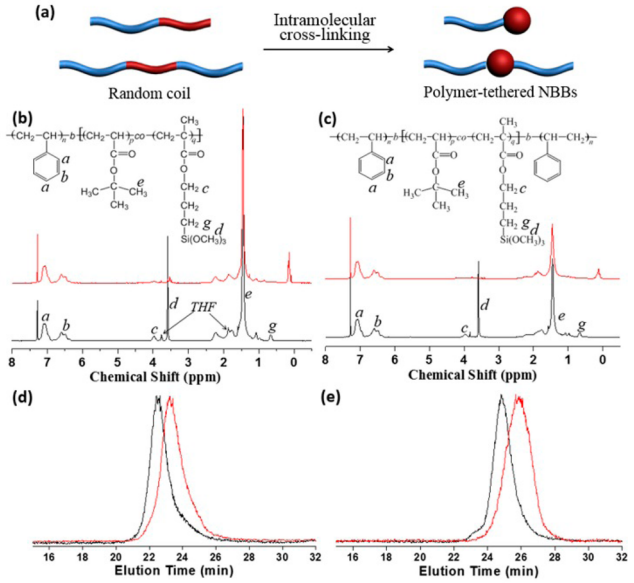

Figure 1. (a) Schematic illustration of polymer-tethered NBBs prepared from linear di-BCPs and tri-BCPs. (b–e) ^{1}H NMR spectra and GPC elution curves of PS_{205}-*b*-P(*t*BA_{174}-*co*-$TMSPMA_{31}$) (b,d) and PS_{99}-*b*-P(*t*BA_{106}-*co*-$TMSPMA_{24}$)-*b*-PS_{99} (c,e) before (black) and after (red) intramolecular cross-linking. The elution curves for NBBs were recorded after hydrolysis for 72 h.

acrylate-*co*-3-(trimethoxysilyl)propyl methacrylate) (P(*t*BA-*co*-TMSPMA)) were prepared. The intramolecular cross-linking of the P(*t*BA-*co*-TMSPMA) block gave rise to the formation of a silica head tethered by one or two PS tails. After deprotection of *tert*-butyl groups on the surface of silica heads, amphiphilic NBBs with a negatively charged hydrophilic silica head and hydrophobic PS tail(s) could be obtained. The effect of polymer chain conformation on the self-assembly of surfactant-mimicking NBBs was carefully investigated.

The linear di-BCPs and tri-BCPs of PS-*b*-P(*t*BA-*co*-TMSPMA) and PS-*b*-P(*t*BA-*co*-TMSPMA)-*b*-PS were prepared by reversible addition–fragmentation chain transfer (RAFT) polymerizations. The synthetic details of BCPs are given in the Supporting Information. To study the effect of the chain conformation of polymer tethers on the self-assembly of NBBs, the repeat unit number of PS-RAFT macrochain-transfer agents for all di-BCPs and tri-BCPs was kept to be ∼200. The intramolecular hydrolysis/polycondensation reaction of TMSPMA moieties was performed in a good solvent for both blocks (e.g., tetrahydrofuran (THF)) with an extremely dilute BCP concentration (0.25 mg/mL) to avoid intermolecular cross-linking. Ammonium hydroxide (10%) was used as a catalyst for the hydrolysis reaction.[34] The intramolecular cross-linking reaction of TMSPMA moieties was first characterized by ^{1}H NMR spectra. Figure 1b shows the ^{1}H NMR spectra of PS_{205}-*b*-P(*t*BA_{174}-*co*-$TMSPMA_{31}$) in $CDCl_3$ before and after intramolecular cross-linking. For linear BCPs, all characteristic peaks of PS blocks (Ar–*H* at 7.1 and 6.6 ppm) and P(*t*BA-*co*-TMSPMA) blocks (–C(CH_3)$_3$ groups of *t*BA units at 1.45 ppm and –OCH_3 groups of TMAPMS at 3.60 ppm) are present, indicating a molecularly dissolved state in $CDCl_3$ before cross-linking. After the intramolecular hydrolysis/polycondensation reactions, the peaks of TMSPMA units at 3.92 ppm (protons of –CH_2OOC– groups, peak *c*), 3.60 ppm (protons of –Si(OCH_3)$_3$ groups, peak *d*), and 0.66 ppm (protons of –SiCH_2– groups, peak *g*) disappeared. Also, the peak intensity of *tert*-butyl groups at 1.45 ppm (peak *e*) decreased by about 20%, suggesting that the P(*t*BA-*co*-TMSPMA) block was locked in a collapsed state in the NBBs. A new peak that appeared at 0.09 ppm was assigned to –SiOSi(CH_3)$_3$ groups from capping reagents. Similar results were observed for tri-BCPs (Figure 1c).

The intramolecular cross-linking was further confirmed by gel permeation chromatography (GPC) measurements.[18] The elution time is known to be determined by the change of hydrodynamic volume of polymer chains. For both di-BCP and tri-BCP, a shift of the GPC peak to a longer elution time was seen. For di-BCP of PS_{205}-*b*-P(*t*BA_{174}-*co*-$TMSPMA_{31}$) (Figure 1d), the apparent number-average molecular weight (M_n) decreased from 72.9 to 60.8 kg/mol after the hydrolysis/polycondensation reaction for 72 h. In the case of tri-BCP of PS_{99}-*b*-P(*t*BA_{106}-*co*-$TMSPMA_{24}$)-*b*-PS_{99} (Figure 1e), a decrease of M_n from 33.2 to 22.7 kg/mol was also present. This corresponded to the decrease in the apparent M_n of P(*t*BA-*co*-TMSPMA) blocks in the di-BCP and tri-BCP approximately to ∼23% and ∼80%, respectively. No other peaks appeared at a shorter elution time. The increase in elution time suggests the decrease in the hydrodynamic size of polymer chains and the occurrence of intramolecular cross-linking (Figures S2 and S3, Supporting Information).

The formation of NBBs can also be visualized using TEM. Figure 2a shows a representative TEM image of NBBs prepared

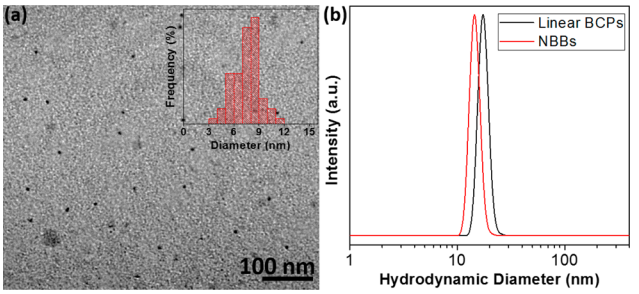

Figure 2. (a) TEM image for NBBs prepared from PS_{205}-*b*-P(*t*BA_{174}-*co*-$TMSPMA_{31}$) in THF. The inset in (a) is the size distribution of polymer-tethered NBBs by averaging more than 150 particles in TEM images. (b) The change in hydrodynamic diameter of PS_{205}-*b*-P(*t*BA_{174}-*co*-$TMSPMA_{31}$) before (black) and after (red) intramolecular cross-linking.

from di-BCP of PS_{205}-*b*-P(*t*BA_{174}-*co*-$TMSPMA_{31}$). The obtained NBBs are nearly spherical and have an average diameter of 7.5 ± 1.5 nm measured from TEM images (see the inset of Figure 2a and Figure S5, Supporting Information). This is consistent with the typical size of previously reported polymer single-chain nanoparticles.[35] Under TEM investigation, the high contrast of NBBs is because of the high electron density of inorganic silica-like NBB heads. Dynamic light scattering (DLS) results in Figure 2b also confirmed the hydrodynamic diameter of linear di-BCPs and NBBs of PS_{205}-*b*-P(*t*BA_{174}-*co*-$TMSPMA_{31}$) to be 18 and 14 nm, respectively. A slightly larger size of NBBs in solution from DLS results was likely attributed to the presence of a PS tail in solution.

A series of di-BCPs of PS-*b*-P(*t*BA-*co*-TMSPMA) and tri-BCPs of PS-*b*-P(*t*BA-*co*-TMSPMA)-*b*-PS with various lengths of P(*t*BA-*co*-TMSPMA) blocks were prepared to study the formation of NBBs. These results are summarized in Table 1. It is interesting to point out that the decrease of all apparent molecular weights of tri-BCPs is larger compared to that of di-

DOI: 10.1021/acsmacrolett.5b00321
ACS Macro Lett. 2015, 4, 736–740

Table 1. Characterizations of Linear BCPs and Polymer-Tethered NBBs

polymers[a]	M_n (kg/mol)[b]	PDI of linear BCPs	M_n (NMR)	TMSPMA: *t*BA (%)[c]	M_n of NBBs (kg/mol)	PDI of NBBs
PS_{205}-RAFT	22.7	1.11			-	-
PS_{205}-*b*-P(*t*BA_{45}-*co*-$TMSPMA_4$)	25.3	1.11	28.1	8.9	24.7	1.09
PS_{205}-*b*-P(*t*BA_{110}-*co*-$TMSPMA_{13}$)	36.9	1.15	38.4	11.8	31.5	1.12
PS_{205}-*b*-P(*t*BA_{120}-*co*-$TMSPMA_{20}$)	41.3	1.26	41.5	16.7	36.1	1.14
PS_{205}-*b*-P(*t*BA_{174}-*co*-$TMSPMA_{31}$)	72.9	1.25	51.1	17.8	60.8	1.18
PS_{205}-*b*-P(*t*BA_{352}-*co*-$TMSPMA_{56}$)	97.1	1.34	79.9	15.9	83.1	1.33
RAFT-PS_{198}-RAFT	20.6	1.12				
PS_{99}-*b*-P(*t*BA_{64}-*co*-$TMSPMA_{23}$)-*b*-PS_{99}	24.1	1.29	34.5	35.8	14.5	1.29
PS_{99}-*b*-P(*t*BA_{106}-*co*-$TMSPMA_{24}$)-*b*-PS_{99}	33.2	1.24	40.1	22.6	22.7	1.22

[a]The repeat unit number of P*t*BA blocks was calculated from ^{1}H NMR spectra based on the molecular weight of the PS block. [b]The number-average molecular weights were determined by GPC calibrated with PS. [c]The TMSPMA content was calculated as its number density in P*t*BA blocks.

BCPs. We hypothesize that (i) a slightly higher content of TMSPMA moieties was present in tri-BCPs and (ii) bitailed BCPs can sterically shield the intramolecularly cross-linked block and stabilize the NBBs better.[24]

Subsequently, the deprotection of *tert*-butyl groups was carried out in the presence of trifluoroacetic acid at room temperature to yield amphiphilic PS-tethered NBBs with hydrophilic silica heads. Again, using PS_{205}-*b*-P(*t*BA_{174}-*co*-$TMSPMA_{31}$) as an example, after deprotection of *tert*-butyl groups, the molecular weight of polymer decreased from 60.8 to 45.6 kg/mol due to the hydrolysis of *tert*-butyl groups (Figure S4a, Supporting Information). This was confirmed by ^{1}H NMR spectra, in which *tert*-butyl groups of P*t*BA blocks at 1.45 ppm disappeared. The obtained NBBs were then comprised of a hydrophilic silica head covered with −COOH groups (denoted as P(AA-*co*-TMSPMA) after the removal of *tert*-butyl groups) and the PS tail (Figure S4b, Supporting Information).

NBBs with a hydrophilic silica head and a hydrophobic PS tail structurally resemble natural surfactant molecules; thus, the self-assembly of such NBBs is expected in a selective solvent. The intramolecular collapse significantly alters the hydrophobic/hydrophilic balance of BCPs that would impact their self-assembly behavior. We first compared the self-assembly of an amphiphilic linear di-BCP of PS_{205}-*b*-PAA_{40} and a NBB of PS_{205}-*b*-P(AA_{45}-*co*-$TMSPMA_4$), of which the length of both blocks was similar (Figure 3a). The self-assembly was triggered by adding water as a selective solvent to the THF solution of

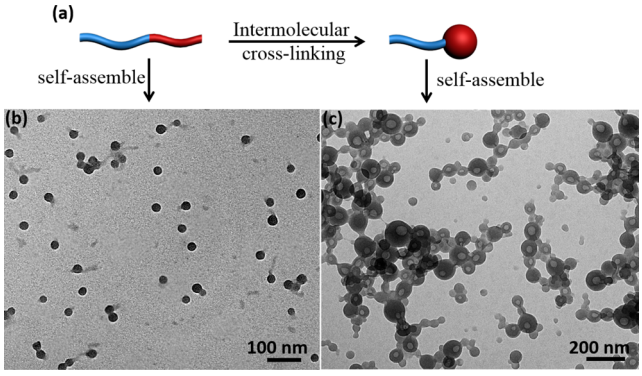

Figure 3. (a) Schematic illustration of the preparation of NBBs from linear BCPs and their self-assembly. (b,c) TEM images of self-assembled morphologies of linear di-BCP of PS_{205}-*b*-PAA_{40} (b) and NBBs prepared from PS_{205}-*b*-P(AA_{45}-*co*-$TMSPMA_4$) (c) in aqueous solution.

linear BCPs or NBBs (see Supporting Information for details). The self-assembly results are given in Figures 3b and c. For the linear di-BCP, spherical micelles with an average diameter of 30 ± 2 nm were obtained, while the NBB of PS_{205}-*b*-P(AA_{45}-*co*-$TMSPMA_4$) assembled dominantly into bilayered vesicles with sizes 80−160 nm. The morphological difference between spherical micelles and bilayered vesicles can be understood as a result of the intermolecular cross-linking of hydrophilic PAA blocks. The decrease in hydrophilic volume fraction would yield less curved assemblies to reduce the interfacial area per chain; therefore, the aggregates changed from spheres to vesicles. This was associated with changing the stretching state of hydrophobic PS. The difference in stretching degree of PS tails (S) in the micelle core and vesicle shell can be characterized by the equation $S = R/R_0$, where R is the radius of PS segments in the micellar aggregates and R_0 is the mean-square end-to-end distance of the PS block. R_0 can be calculated from $R_0 = b \times (N_{PS}/6.92)^{0.5}$, where b is the length of Kuhn monomers (b = 1.8 nm for PS) and N_{PS} is the number of PS blocks.[36] R_0 is equal to 9.8 nm for N_{PS} of 205. The stretching degree of PS blocks in linear BCPs and NBBs is 1.6 and 1.1, respectively (Figures S6−7, Supporting Information). In the case of spherical micelles, the conformational entropy penalty from the stretching PS tails was balanced out by reducing the repulsion force between hydrophilic PAA blocks.

The influence of the size of the hydrophilic silica head on the self-assembled aggregates was also studied at a fixed PS tether length. We observed a morphological evolution from bilayered vesicles in Figure 4a to spherical micelles in Figures 4b and c by varying the molecular weight of the P(*t*BA-*co*-TMSPMA) block from 2.6 to 74.4 kg/mol (also see Figures S7−8, Supporting Information). The overall dimension of micellar aggregates decreased from 128 to 23 nm by increasing the size of hydrophilic silica heads of NBBs, also confirmed by dynamic light scattering. This result is similar to the linear BCP of PS-*b*-PAA where the size of micellar cores scales in a power law described by $R_{core} \sim N_{PS}^{0.4} N_{PAA}^{-0.15}$.[37] The volume increase of hydrophilic silica heads resulted in the increase of the repulsive interactions among hydrophilic heads; thus, the formation of aggregates with a larger interfacial curvature was expected. It should be noted that spherical aggregates with surface protrusions were obtained for NBBs of PS_{205}-*b*-P(*t*BA_{352}-*co*-$TMSPMA_{56}$) (Figure 4c). The formation of these protrusions is probably because of the presence of large hydrophilic silica-like heads. The topological features of spherical micelles are known as virus-mimicking structures that may benefit biomimetic drug delivery studies.[38]

DOI: 10.1021/acsmacrolett.5b00321
ACS Macro Lett. 2015, 4, 736−740

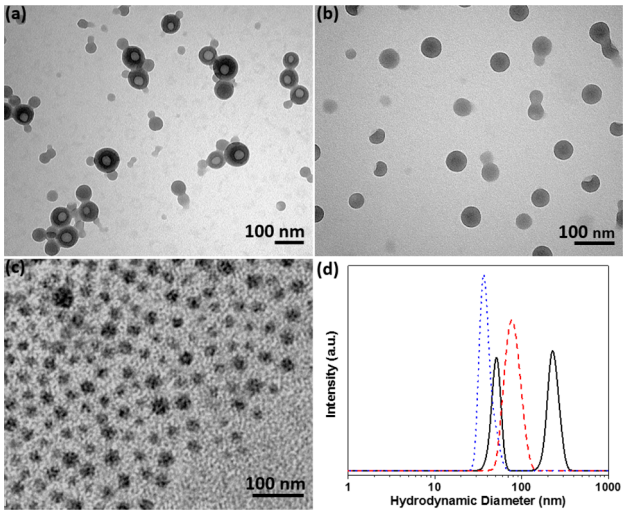

Figure 4. Representative TEM images of self-assembled morphologies of NBBs with different hydrophilic heads: (a) PS_{205}-*b*-P(AA_{45}-*co*-$TMSPMA_4$), (b) PS_{205}-*b*-P(AA_{120}-*co*-$TMSPMA_{20}$), and (c) PS_{205}-*b*-P(AA_{352}-*co*-$TMSPMA_{56}$). (d) Hydrodynamic diameter of self-assembled morphologies of NBBs: PS_{205}-*b*-P(AA_{45}-*co*-$TMSPMA_4$) (black line), PS_{205}-*b*-P(AA_{174}-*co*-$TMSPMA_{31}$) (red dash line), and PS_{205}-*b*-P(AA_{352}-*co*-$TMSPMA_{56}$) (blue dot line).

Given "ABA" tri-BCPs with two PS blocks at each end of a P(*t*BA-*co*-TMSPMA) block, the intramolecular cross-linking would yield NBBs with two hydrophobic PS tails. This makes it possible to study the effect of the number of polymer tethers on the self-assembly of NBBs. To do so, the single-tailed NBB of PS_{205}-*b*-P(AA_{110}-*co*-$TMSPMA_{13}$) and bitailed NBB of PS_{99}-*b*-P(AA_{106}-*co*-$TMSPMA_{24}$)-*b*-PS_{99} were prepared by keeping the same hydrophobic volume fraction of NBBs. The micellar aggregates were investigated by TEM as given in Figure 5 and

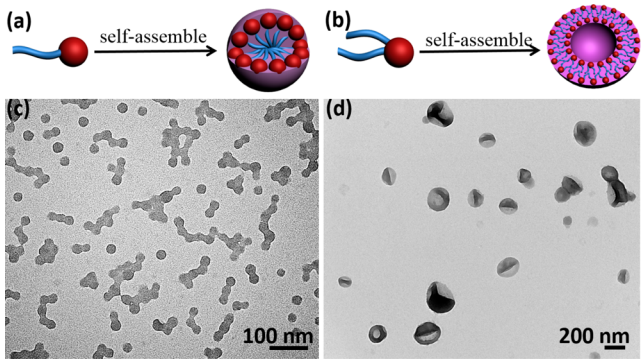

Figure 5. (a,b) Schematic illustration of single-tailed and bitailed NBBs. (c,d) TEM images of self-assembly morphologies of NBBs prepared from (c) PS_{205}-*b*-P(AA_{110}-*co*-$TMSPMA_{13}$) and (d) PS_{99}-*b*-P(AA_{97}-*co*-$TMSPMA_{31}$)-*b*-PS_{99}.

Figure S9 (Supporting Information). Bilayered vesicles with an average diameter of ~300 nm were observed for bitailed NBBs of PS_{99}-*b*-P(AA_{106}-*co*-$TMSPMA_{24}$)-*b*-PS_{99}, while only spherical micelles with an average size of 24 ± 3 nm were obtained for single-tailed NBBs of PS_{205}-*b*-P(AA_{110}-*co*-$TMSPMA_{13}$). The conformational entropy of hydrophobic PS tails is believed to be critical in controlling the morphological change. If assuming that the hydrophilic heads of both NBBs are close (~4.5 nm), the "effective" hydrophobic volume varies with the number of PS tails. A single PS tail having a much smaller cross-section area compared to hydrophilic heads can easily be stretched to form a wedge-like shape.[8] On the contrary, bitailed NBBs topologically have more space requirements and hold a cylindrical shape where the hydrophobic cross-sectional area is larger.[39] Therefore, the increase in hydrophobic volume by altering the conformation of polymer tethers leads to the formation of vesicles for bitailed NBBs.

Quantitatively, the wall thickness of vesicles prepared from the bitailed NBB of PS_{99}-*b*-P(tBA_{106}-*co*-$TMSPMA_{24}$)-*b*-PS_{99} is 25 ± 4 nm, close to the size of the micelle prepared from the single-tailed NBB of PS_{205}-*b*-P(tBA_{110}-*co*-$TMSPMA_{13}$). The stretching degree of PS tails can be estimated to be 1.8 for bitailed NBB and 1.2 for single-tailed NBB, respectively (Table S1, Supporting Information); that is, the PS tails are highly stretched in the vesicles formed by bitailed NBB. This result is quite different from that of amphiphilic linear BCPs previously reported by Bates[40,41] and Eisenberg.[37,42] In the case of BCP vesicles, the stretching of hydrophobic blocks was not observed because a decrease in the interfacial curvature of vesicles would reduce the interfacial area per chain, and the associated entropic penalty also increased with longer, stretched hydrophobic blocks. However, for the bitailed NBB, the topological nanostructures likely play a role here. The two coiled PS tails on the sides of a silica head in NBBs were expected to be slightly stretched in the course of the self-assembly where the hydrophilic heads could be exposed to the solvent, thus stabilizing the assemblies (Figure 5b).

In summary, we have prepared a series of surfactant-mimicking NBBs with a hydrophilic charged head and one (or two) hydrophobic fatty tail(s) and studied their self-assemblies in aqueous solution. Using "AB" di-BCPs and "ABA" tri-BCPs of PS and P(*t*BA-*co*-TMSPMA), the intramolecular folding of P(*t*BA-*co*-TMSPMA) blocks and the deprotection of *tert*-butyl groups were demonstrated to be an efficient method to prepare amphiphilic NBBs with a hydrophilic silica head tethered by one or two PS tails. The self-assembly of these amphiphilic NBBs was further studied by fixing the molecular weight of PS tails and varying the size of the hydrophilic heads. The intrachain cross-linking of hydrophilic heads that shifted the hydrophilic/hydrophobic balance of polymers resulted in morphological transitions from bilayered vesicles to spherical micelles. Surface protrusions were found for spherical micelles prepared from NBBs with large hydrophilic heads. We also found the chain conformation of PS tails to be critical for the self-assembly of NBBs, where the bitailed NBBs with highly stretched PS tails favored bilayered vesicle structures. These results offer new insight into nanostructure-determined self-assembly of NBBs that may provide a new pathway to control the self-assembly of NBBs in solution.

■ ASSOCIATED CONTENT

Supporting Information

Synthetic details of BCPs/NBBs and additional GPC/TEM characterizations. The Supporting Information is available free of charge on the ACS Publications website at DOI: 10.1021/acsmacrolett.5b00321.

■ AUTHOR INFORMATION

Corresponding Author

*Tel.: +1-860-486-2744. E-mail: jie.he@uconn.edu.

Notes

The authors declare no competing financial interest.

DOI: 10.1021/acsmacrolett.5b00321
ACS Macro Lett. 2015, 4, 736−740

■ ACKNOWLEDGMENTS

JH is grateful for the financial support of startup funds from the University of Connecticut. The authors thank Prof. Vijay Kumar for the DLS measurements. This work was also partially supported by the Green Emulsions Micelles and Surfactants (GEMS) Center.

■ REFERENCES

(1) Zhang, K.; Jiang, M.; Chen, D. *Prog. Polym. Sci.* **2012**, *37*, 445.
(2) Fernandes, N. J.; Koerner, H.; Giannelis, E. P.; Vaia, R. A. *MRS Commun.* **2013**, *3*, 13.
(3) Glotzer, S. C. *Science* **2004**, *306*, 419.
(4) Moffitt, M. G. *J. Phys. Chem. Lett.* **2013**, *4*, 3654.
(5) Zhang, W.-B.; Yu, X.; Wang, C.-L.; Sun, H.-J.; Hsieh, I. F.; Li, Y.; Dong, X.-H.; Yue, K.; Van Horn, R.; Cheng, S. Z. D. *Macromolecules* **2014**, *47*, 1221.
(6) Guo, Y.; Harirchian-Saei, S.; Izumi, C. M. S.; Moffitt, M. G. *ACS Nano* **2011**, *5*, 3309.
(7) Hu, J.; Wu, T.; Zhang, G.; Liu, S. *J. Am. Chem. Soc.* **2012**, *134*, 7624.
(8) Yu, X.; Zhang, W. B.; Yue, K.; Li, X.; Liu, H.; Xin, Y.; Wang, C. L.; Wesdemiotis, C.; Cheng, S. Z. *J. Am. Chem. Soc.* **2012**, *134*, 7780.
(9) Nie, Z.; Fava, D.; Kumacheva, E.; Zou, S.; Walker, G. C.; Rubinstein, M. *Nat. Mater.* **2007**, *6*, 609.
(10) Song, J.; Cheng, L.; Liu, A.; Yin, J.; Kuang, M.; Duan, H. *J. Am. Chem. Soc.* **2011**, *133*, 10760.
(11) Zhang, Z. L.; Horsch, M. A.; Lamm, M. H.; Glotzer, S. C. *Nano Lett.* **2003**, *3*, 1341.
(12) Glotzer, S. C.; Solomon, M. J. *Nat. Mater.* **2007**, *6*, 557.
(13) Ouchi, M.; Badi, N.; Lutz, J. F.; Sawamoto, M. *Nat. Chem.* **2011**, *3*, 917.
(14) Terashima, T.; Mes, T.; De Greef, T. F. A.; Gillissen, M. A. J.; Besenius, P.; Palmans, A. R. A.; Meijer, E. W. *J. Am. Chem. Soc.* **2011**, *133*, 4742.
(15) Huerta, E.; Stals, P. J. M.; Meijer, E. W.; Palmans, A. R. A. *Angew. Chem., Int. Ed.* **2013**, *52*, 2906.
(16) He, J.; Tremblay, L.; Lacelle, S.; Zhao, Y. *Soft Matter* **2011**, *7*, 2380.
(17) Perez-Baena, I.; Loinaz, I.; Padro, D.; Garcia, I.; Grande, H. J.; Odriozola, I. *J. Mater. Chem.* **2010**, *20*, 6916.
(18) Harth, E.; Van Horn, B.; Lee, V. Y.; Germack, D. S.; Gonzales, C. P.; Miller, R. D.; Hawker, C. J. *J. Am. Chem. Soc.* **2002**, *124*, 8653.
(19) Gauthier, M. A.; Gibson, M. I.; Klok, H.-A. *Angew. Chem., Int. Ed.* **2009**, *48*, 48.
(20) Cherian, A. E.; Sun, F. C.; Sheiko, S. S.; Coates, G. W. *J. Am. Chem. Soc.* **2007**, *129*, 11350.
(21) Hosono, N.; Gillissen, M. A. J.; Li, Y.; Sheiko, S. S.; Palmans, A. R. A.; Meijer, E. W. *J. Am. Chem. Soc.* **2013**, *135*, 501.
(22) Pomposo, J. A.; Perez-Baena, I.; Lo Verso, F.; Moreno, A. J.; Arbe, A.; Colmenero, J. *ACS Macro Lett.* **2014**, *3*, 767.
(23) Moreno, A. J.; Lo Verso, F.; Sanchez-Sanchez, A.; Arbe, A.; Colmenero, J.; Pomposo, J. A. *Macromolecules* **2013**, *46*, 9748.
(24) Wong, E. H. H.; Qiao, G. G. *Macromolecules* **2015**, *48*, 1371.
(25) Wen, J.; Zhang, J.; Zhang, Y.; Yang, Y.; Zhao, H. *Polym. Chem.* **2014**, *5*, 4032.
(26) Cheng, L.; Hou, G.; Miao, J.; Chen, D.; Jiang, M.; Zhu, L. *Macromolecules* **2008**, *41*, 8159.
(27) Zhou, F.; Xie, M.; Chen, D. *Macromolecules* **2014**, *47*, 365.
(28) Beck, J. B.; Killops, K. L.; Kang, T.; Sivanandan, K.; Bayles, A.; Mackay, M. E.; Wooley, K. L.; Hawker, C. J. *Macromolecules* **2009**, *42*, 5629.
(29) Hansell, C. F.; Lu, A.; Patterson, J. P.; O'Reilly, R. K. *Nanoscale* **2014**, *6*, 4102.
(30) Altintas, O.; Willenbacher, J.; Wuest, K. N. R.; Oehlenschlaeger, K. K.; Krolla-Sidenstein, P.; Gliemann, H.; Barner-Kowollik, C. *Macromolecules* **2013**, *46*, 8092.
(31) Dirlam, P. T.; Kim, H. J.; Arrington, K. J.; Chung, W. J.; Sahoo, R.; Hill, L. J.; Costanzo, P. J.; Theato, P.; Char, K.; Pyun, J. *Polym. Chem.* **2013**, *4*, 3765.
(32) Lyon, C. K.; Prasher, A.; Hanlon, A. M.; Tuten, B. T.; Tooley, C. A.; Frank, P. G.; Berda, E. B. *Polym. Chem.* **2015**, *6*, 181.
(33) Li, W.; Kuo, C.-H.; Kanyo, I.; Thanneeru, S.; He, J. *Macromolecules* **2014**, *47*, 5932.
(34) Du, J.; Chen, Y. *Macromolecules* **2004**, *37*, 5710.
(35) Cherian, A. E.; Sun, F. C.; Sheiko, S. S.; Coates, G. W. *J. Am. Chem. Soc.* **2007**, *129*, 11350.
(36) Rubinstein, M.; Colby, R. *Polymers Physics*; Oxford: Oxford, U.K., 2003.
(37) Zhang, L.; Eisenberg, A. *J. Am. Chem. Soc.* **1996**, *118*, 3168.
(38) Van Lehn, R. C.; Ricci, M.; Silva, P. H.; Andreozzi, P.; Reguera, J.; Voïtchovsky, K.; Stellacci, F.; Alexander-Katz, A. *Nat. Commun.* **2014**, *5*, 4482.
(39) Ma, S.; Hu, Y.; Wang, R. *Macromolecules* **2015**, *48*, 3112.
(40) Won, Y.-Y.; Brannan, A. K.; Davis, H. T.; Bates, F. S. *J. Phys. Chem. B* **2002**, *106*, 3354.
(41) Miller, R. *Giant Micelles: Properties and Applications*; CRC Press: Boca Raton, FL, 2007; Vol. *140*.
(42) Zhang, L.; Eisenberg, A. *Polym. Adv. Technol.* **1998**, *9*, 677.

DOI: 10.1021/acsmacrolett.5b00321
ACS Macro Lett. 2015, 4, 736−740